

Magnetic Phase Diagram of Lightly Doped $\text{La}_{2-x}\text{Sr}_x\text{CuO}_4$ from ^{139}La Nuclear Quadrupole Resonance

F. C. Chou,¹ F. Borsa,^{1,2} J. H. Cho,^{1,*} D. C. Johnston,¹ A. Lascialfari,² D. R. Torgeson,¹ and J. Ziolo¹

¹Ames Laboratory and Department of Physics and Astronomy, Iowa State University, Ames, Iowa 50011

²Dipartimento di Fisica "A. Volta," Università di Pavia, I-27100 Pavia, Italy

(Received 2 March 1993; revised manuscript received 7 July 1993)

The magnetic phase diagram of $\text{La}_{2-x}\text{Sr}_x\text{CuO}_4$ in the antiferromagnetic regime ($x \leq 0.02$) has been derived from ^{139}La nuclear quadrupole resonance studies from 4 to 250 K. The data demonstrate freezing of the doped holes' effective spin degrees of freedom below $T_f \approx (815 \text{ K})x$ into a spin-glass-like state which is superimposed on the antiferromagnetic background. These and previous results allow a detailed magnetic phase diagram to be constructed for $x \leq 0.05$ and reveal a distinct crossover at $x \approx 0.02$ in the nature of the spin-glass transition.

PACS numbers: 75.30.Kz, 74.25.Nf, 74.72.Dn, 76.60.Gv

The introduction of holes in the CuO_2 plane by Sr doping in $\text{La}_{2-x}\text{Sr}_x\text{CuO}_4$ is known to reduce drastically the Néel temperature $T_N \approx 300 \text{ K}$ of the planar Heisenberg antiferromagnet (AF) La_2CuO_4 , whereby T_N decreases to 0 K by $x \approx 0.02$. Throughout the low doping regime, $x < 0.08$, a rich phenomenology is observed below $\sim 20 \text{ K}$ with anomalies in ^{139}La nuclear quadrupole resonance (NQR) relaxation rate [1,2], muon spin rotation (μSR) [3,4], neutron scattering [4], and magnetic susceptibility $\chi(T)$ and electron spin resonance (ESR) [5] measurements, which have been attributed to a low temperature magnetic phase similar to a spin glass (SG) [3–5]. In the "spin-glass regime," $0.02 \leq x \leq 0.08$, Cho *et al.* have recently inferred from ^{139}La NQR data that this phase is a cluster spin glass [1]. In the AF regime $x \leq 0.02$, on the other hand, the origin of these anomalies below T_N is obscure, although similarities in behavior to so-called reentrant spin-glass systems [6] have been noted [3,7].

In this Letter, we report a detailed ^{139}La NQR investigation from 4 to 250 K in the AF regime ($x \leq 0.02$) of $\text{La}_{2-x}\text{Sr}_x\text{CuO}_4$. The static data show anomalous changes below $\sim 30 \text{ K}$. The central results of this paper are seen in the dynamics. We find that the effective spin degree(s) of freedom associated with the doped holes freeze below a temperature $T_f \approx (815 \text{ K})x$, corresponding to $T_f \approx 16 \text{ K}$ for $x = 0.02$. This spin freezing is superimposed on the background long-range AF order of the Cu^{+2} spins in the CuO_2 planes, and does not significantly affect the effective local internal magnetic field at the La sites. Together with results from previous $\chi(T)$ data for $0 \leq x \leq 0.03$ [8] and ^{139}La NQR data for $0.02 \leq x \leq 0.08$ [1] of Cho *et al.*, a detailed magnetic phase diagram is constructed for $0 \leq x \leq 0.05$. A crossover in the nature of the SG transition at $x \approx 0.02$ is clearly indicated by the totality of the data; an interpretation is given and discussed in the context of related theoretical predictions.

Single phase samples of $\text{La}_{2-x}\text{Sr}_x\text{CuO}_4$ were prepared by solid state reaction and annealed in 1 bar O_2 , and were the same as used previously in Refs. [1] and [8]. The ^{139}La ($I = \frac{7}{2}$) NQR measurements were performed at

both the $3\nu_Q$ and $2\nu_Q$ transitions with a pulse Fourier transform spectrometer ($\nu_Q \approx 6.3 \text{ MHz}$).

The static ^{139}La NQR results from the $2\nu_Q$ line for several of the $\text{La}_{2-x}\text{Sr}_x\text{CuO}_4$ samples are summarized in Figs. 1(a)–1(c). From $\chi(T)$ data [8], $T_N = 227, 209, 194, 164,$ and 122 K for $x = 0.008, 0.010, 0.012, 0.014,$ and 0.016 , respectively. Below T_N , the ^{139}La NQR splits into a doublet at frequencies ν_1 and ν_2 whose separation $\Delta\nu$ [see Fig. 1(c)] measures the component $H_z = H \cos\theta$ of the static effective local internal magnetic field \mathbf{H} at the La site parallel to the principal (z) axis of the electric field gradient (EFG) tensor; $\theta = 78^\circ$ in La_2CuO_4 and the z axis is nearly perpendicular to the CuO_2 planes [9]. The two NQR resonance frequencies in the doublet are given by $\nu_{1,2} = 2\nu_Q \pm (\gamma_N/2\pi)H_z$, where the quadrupole frequency $\nu_Q \approx 6.3 \text{ MHz}$ and $\gamma_N/2\pi = 601.44 \text{ Hz/G}$ is the nuclear gyromagnetic ratio. For $x > 0$ and decreasing T below $\sim 30 \text{ K}$, $\nu_1 + \nu_2 = 4\nu_Q$ shows an anomalous decrease [Fig. 1(a)], and the NQR linewidth (FWHM) [Fig. 1(b)] and $\nu_1 - \nu_2 = 2(\gamma_N/2\pi)H_z$ [Fig. 1(c)] display anomalous increases; at 4.2 K , $\text{FWHM}(x) \approx 8x + 0.06 \text{ MHz}$. The line broadening for the $3\nu_Q$ transition (not shown) is about 50% more pronounced than for the $2\nu_Q$ transition in Fig. 1(b), indicating a quadrupolar rather than a magnetic broadening mechanism. The anomalous behaviors of the EFG reflected in Figs. 1(a) and 1(b) below $\sim 30 \text{ K}$ could arise from an onset below 30 K of a small incoherent or incommensurate (or long-period commensurate) modulation of the oxygen positions and/or from the localization of the doped holes, as deduced from ac and dc resistivity measurements [10], below this T .

Figure 1(c) demonstrates that H_z increases dramatically below $\sim 30 \text{ K}$ for the larger x values, compared to the behavior for $x = 0$. Remarkably, in spite of this behavior, $H_z(T=0) \approx 210 \text{ G}$ is nearly independent of x (and T_N). The change ΔH_z in $H_z = H \cos\theta$ below 30 K could arise from a change in θ , in H , or in both. However, because $H_z(T=0)$ is unaffected by doping, it seems most likely that the observed $\Delta H_z(T)$ is caused by corresponding changes in H . This hypothesis is supported by recent ESR measurements of Gd probe spins in a sample

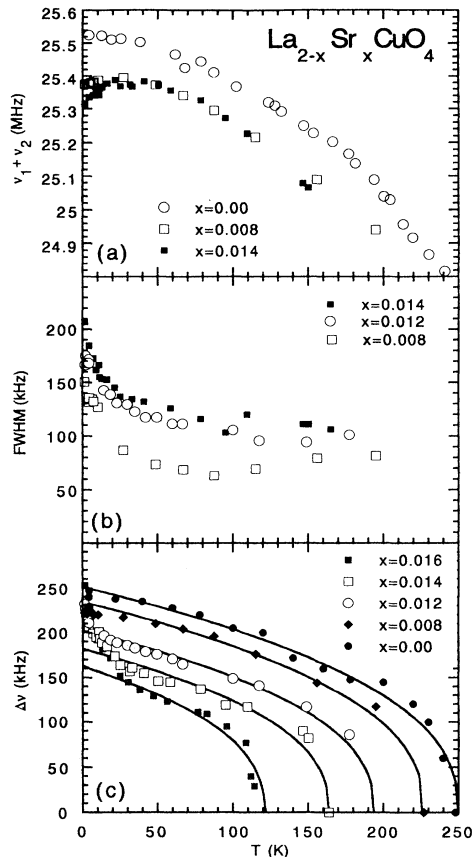


FIG. 1. Temperature (T) dependence of the ^{139}La NQR in $\text{La}_{2-x}\text{Sr}_x\text{CuO}_4$. (a) Sum of frequencies ν_1 and ν_2 vs T . (b) Full width at half maximum (FWHM) vs T of each individual NQR line in the doublet. (c) Splitting $\Delta\nu = \nu_2 - \nu_1$ vs T . The full curves represent a fit of the data with a power law $(1 - T/T_N)^\beta$, with $\beta = 0.40 \pm 0.01$ and $T_N(x)$ chosen according to the phase diagram. For $x \neq 0$ only the data for $T > 30$ K are included in the fit.

with Sr doping level $x = 0.009$, which showed an increase in H below ≈ 20 K [11]. On the other hand, μSR measurements of $\text{La}_2\text{CuO}_{4+\delta}$ and $\text{La}_{2-x}\text{Sr}_x\text{CuO}_4$ samples with T_N values from ~ 100 to 300 K do not show such anomalous changes in the local magnetic field at the muon site below 30 K; however, the local field at $T = 0$ is found to be nearly independent of T_N [3,5,12], as found here. In contrast, neutron diffraction studies show a nearly proportional decrease in the ordered moment at $T = 0$ with decreasing T_N [13]; two of these studies show a *decrease* in the ordered moment below ~ 30 K [14], whereas others show no anomalous changes [12].

The central results of this paper are contained in the observed dynamics of the ^{139}La nuclei in $\text{La}_{2-x}\text{Sr}_x\text{CuO}_4$ ($x < 0.02$). We emphasize that a study of the NQR line intensities vs x and T showed that all or almost all of the La nuclei participate in the nuclear spin-lattice relaxation rate (NSLR), R_1 , behaviors described here. The decays of both the transverse nuclear magnetization (a T_2 pro-

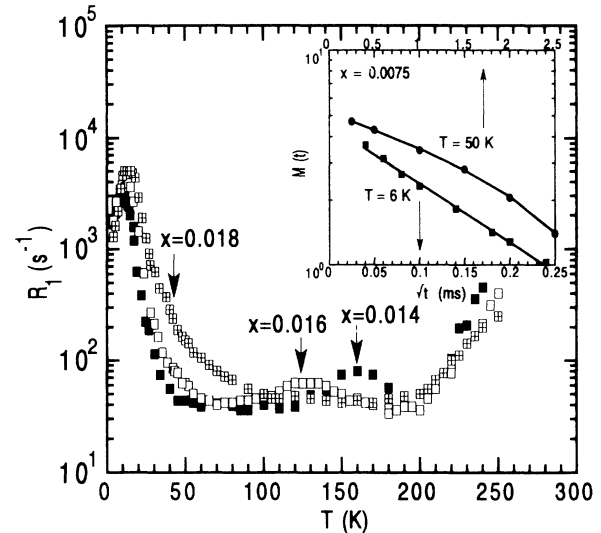


FIG. 2. Temperature dependence of R_1 of the ^{139}La NQR transition at $3\nu_Q$ in $\text{La}_{2-x}\text{Sr}_x\text{CuO}_4$. The increase of R_1 from 200 to 250 K results from the diffusion of excess oxygen within the sample. The arrows denote $T_N(x)$ as determined from $\chi(T)$ [8] and NQR results ($x = 0.018$). The inset shows the crossover from a Gaussian (at 50 K) to an exponential \sqrt{t} behavior (at 6 K) of the transverse magnetization decay in a sample with $x = 0.0075$. The error bars in the inset are the size of the data symbols; the upper curve is a guide to the eye, and the lower straight line is a least squares fit to the data at 6 K.

cess) and the longitudinal magnetization in a two pulse echo experiment change from almost Gaussian above 30 K to an exponential \sqrt{t} dependence at lower T for all samples for both the $2\nu_Q$ and $3\nu_Q$ transitions, as illustrated in the inset in Fig. 2 for the former decay. Therefore, below 30 K the R_1 data presented here are effective rates determined from this decay law [$R_1 \equiv 1/T_1^*$, see Eq. (1) below], whereas above 30 K R_1 was determined from the initial recovery of the nuclear magnetization $M(t)$ after a short ($\tau \ll R_1^{-1}$) saturating sequence. The R_1 data for the $3\nu_Q$ transition, shown in Fig. 2, exhibit a weak peak associated with the AF ordering at the same T_N as obtained from $\chi(T)$ results. In addition, R_1 displays a strong peak at a temperature $T_f < 16$ K which is proportional to x : $T_f = (815 \text{ K})x$ (see Fig. 4 below).

For a magnetic relaxation mechanism described by a relaxation transition probability W , one has $R_1 \approx 23 W$ for the $3\nu_Q$ line and $R_1 \approx 41 W$ for the $2\nu_Q$ line, yielding $R_1(2\nu_Q)/R_1(3\nu_Q) = 1.78$. This value is the same within the errors as our experimental value 1.89 ± 0.15 for $x = 0.014$. Further, from Figs. 1(a) and 1(b), there are no observable features in ν_Q or in the linewidth associated with the temperature T_f . These findings provide strong evidence that the peak in R_1 at T_f is of magnetic, and not structural, origin. We conclude that the peak in R_1 at T_f arises from a magnetic mechanism, in agreement with previous work [2].

The time dependence of the magnetization recovery

below 30 K,

$$M(\infty) - M(t) \propto \exp[-(t/T_f^*)^{1/2}], \quad (1)$$

implies a distribution of relaxation times as expected in the presence of a distribution of localized moment relaxing centers with diffusionless relaxation of the ^{139}La nuclei to the impurities (no common spin temperature) [15]. One can prove that $R_1 \equiv (T_f^*)^{-1} = 2(\bar{T}_1)^{-1}$, where \bar{T}_1 is the relaxation time averaged over the distribution [16]. In order to relate $(T_f^*)^{-1}$ to the hole concentration and spin dynamics, we assume that the W of a ^{139}La nucleus at distance r from a localized hole's effective spin is given by the dipolar interaction: $23W(r) = (A/r^6)\tau$. Here, A is the dipolar coupling constant and τ is the autocorrelation time of the effective spin. For negligible nuclear-spin diffusion, the $M(t)$ is an ensemble average over all possible hole spin configurations about a given nuclear site. For $x \ll 1$ and $(A/r_0^6)\tau t \gg 1$, where r_0 is the minimum distance between a ^{139}La nucleus and a hole spin, one then finds Eq. (1), with [15]

$$R_1 \equiv (T_f^*)^{-1} \approx (4N_0\pi^{3/2}/3)^2 x^2 A\tau, \quad (2)$$

where N_0 is the number of available hole sites per unit volume. For $x \ll 1$, the correlation time τ , which depends on the interaction which couples the localized hole spins, scales as $\tau \propto x^{-1}$ [15] and predicts $R_1 \propto x$ in Eq. (2). In the presence of spin freezing one expects a slowing down of τ with decreasing T , leading to an enhancement of the NSLR according to Eq. (2). Phase-transition theories predict $\tau \propto (T - T_f)^{-n}$, whereas nonequilibrium models predict an Arrhenius law, $\tau = \tau_0 \exp(E/k_B T)$ [17]. The

two predictions are compared with the data in Fig. 3. On the basis of the present data and fits in Fig. 3, we cannot clearly distinguish whether a true phase transition or a continuous freezing occurs at T_f . In either the phase transition or activated models for τ above, in order to account for the very large NSLR at T_f , we infer that τ^{-1} reaches the MHz range. In the presence of a distribution of correlation times, one expects a broad and asymmetric maximum of $\ln(R_1)$ vs $1/T$, as seen in Fig. 3, with the average correlation time $\tau \approx (2\pi\nu_Q)^{-1}$ at the maximum [17]. This expression for τ , the data in Fig. 2, and Eq. (2) yield $A \sim 10^{-31} \text{ rad}^2 \text{ sec}^{-2} \text{ cm}^6$, which is of the order of magnitude expected for a dipolar interaction of a ^{139}La nucleus with a hole moment of about $1\mu_B$. This supports the validity of Eq. (2) and the discussion relating to it.

We conclude that the peaks in R_1 at T_f arise from freezing of the effective spin degrees of freedom associated with the doped holes. Examination of Fig. 1(c) shows that this spin freezing is independent of the effective magnetic field H_z at the La site, and therefore of the (longitudinal) Cu^{+2} spin degrees of freedom which order below T_N . ESR measurements [5] have previously indicated that the doped holes possess independent spin degrees of freedom.

As noted above and shown in Fig. 4, T_f is proportional to x with a large slope: $T_f = (815 \text{ K})x$. In the context of known reentrant or conventional spin glasses, both features are remarkable. In Fig. 4, there is no discernible threshold in x for spin freezing, in contrast to the usual case where a percolation threshold must first be exceeded. This indicates that the effective interaction between the effective doped hole spins is of long range and that mean

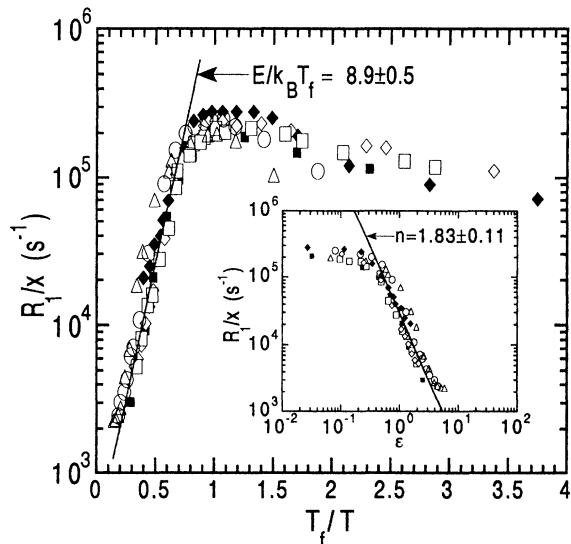


FIG. 3. A common behavior for all concentrations is demonstrated by $R_1(x, T)/x$ vs T_f/T . The straight line defines an activated behavior $\tau \propto \exp(E/k_B T)$. The inset shows R_1/x vs $\epsilon = (T - T_f)/T_f$. The straight line corresponds to a critical behavior $\tau \propto \epsilon^{-n}$.

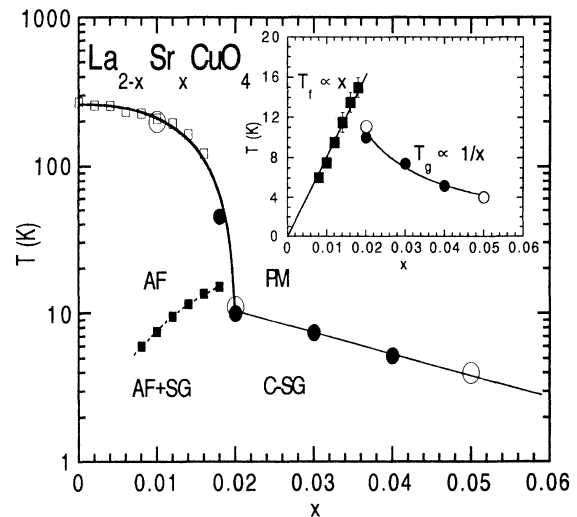


FIG. 4. Magnetic phase diagram of $\text{La}_{2-x}\text{Sr}_x\text{CuO}_4$. The closed squares and circles are from NQR, the open squares from $\chi(T)$ [8], and the open circles from μSR [3]. The inset shows T_f and T_g vs x . Abbreviations: PM (paramagnetic), AF (antiferromagnetic), SG (spin glass), and CSG (cluster spin glass).

field theory should be applicable, consistent with $T_f \propto x$. The slope $T_f/x = 815$ K is comparable to the exchange interaction (≈ 1500 K) between adjacent Cu atoms in the CuO_2 planes, suggesting that the doped hole spin interaction is indirect and mediated by the AF Cu spin system. Indeed, recent microscopic theory [18,19] predicts that localized holes couple to each other via a long range perturbation induced in the AF background, leading to freezing of the holes' effective spins with $T_f \propto x$; the predicted T_f values [18,19] are close to our observed ones. In Ref. [18], the spin degrees of freedom associated with the doped holes are the transverse (out-of-plane) components of the Cu spins near the hole which are induced by the presence of the hole on a plaquette of four oxygen ions. This is consistent with our data, which indicate that the spin degrees of freedom associated with the doped holes are distinct from the (longitudinal) Cu^{+2} spin degree of freedom which orders below T_N . It is apparently the localization of the doped holes below ~ 50 K [10] which allows for subsequent observation of ordering of their spin degrees of freedom below T_f . Delocalization of the holes above T_f is predicted [18] to reduce the local magnetic field at the La sites relative to the value for localized holes; this may be the cause of the anomalous behavior below 30 K in Fig. 1(c).

By combining the present with the previous [1,8] results, a detailed magnetic phase diagram for lightly doped ($0 \leq x \leq 0.05$) $\text{La}_{2-x}\text{Sr}_x\text{CuO}_4$ was constructed and is shown in Fig. 4, where the spin-glass freezing temperature for $x > 0.02$ [1] is denoted by T_g . From Fig. 4, a distinct crossover at $x \approx 0.02$ occurs in the composition dependence of the freezing temperature: $T_f \propto x$ for $x < 0.02$, whereas $T_g \propto 1/x$ for $x > 0.02$. This novel behavior indicates that there is a crossover at $x = 0.02$ in the nature of the spin-glass transition. According to the above discussion, for $x < 0.02$ the transition at T_f should be viewed as the freezing of the spin degrees of freedom associated with the doped holes, superimposed on the preexisting AF long-range order. For $x > 0.02$, on the other hand, the system undergoes a collective phase transition from a paramagnetic state, with 2D dynamical correlations in undoped mesoscopic domains of size $L \propto 1/\sqrt{x}$, to a cluster-spin-glass (CSG) phase in which these domains freeze due to their mutual interaction [1]; a static internal magnetic field occurs only below T_g [1]. By using the molecular field approximation result, $T_g \approx J'(\xi_{2D}/a)^2$, where J' is the effective Cu-Cu interplane coupling and $a = 3.8 \text{ \AA}$ is the intraplane Cu-Cu distance, one expects $T_g \propto L^2 \propto 1/x$, as in Fig. 4, for a system where the intraplane AF correlation length ξ_{2D} is limited to a finite size L ; from the data in Fig. 4, $J' \approx 0.2$ K. ^{139}La NQR measurements vs x at 1.4 K, not presented here, suggest a different spin structure in the AF plus SG and the CSG regions of the phase diagram; further experiments are needed to determine if a phase boundary ex-

ists.

The authors wish to thank A. Rigamonti and R. J. Gooding for useful discussions. Ames Laboratory is operated for the U.S. Department of Energy by Iowa State University under Contract No. W-7405-Eng-82. The work at Ames was supported by the Director for Energy Research, Office of Basic Energy Sciences.

*Present address: MS K763, Los Alamos National Laboratory, Los Alamos, NM 87545.

- [1] J. H. Cho, F. Borsa, D. C. Johnston, and D. R. Torgeson, *Phys. Rev. B* **46**, 3179 (1992).
- [2] A. Rigamonti *et al.*, in *Earlier and Recent Aspects of Superconductivity*, edited by J. G. Bednorz and K. A. Müller (Springer, Berlin, 1990). See also A. V. Zalesskii *et al.*, *Superconductivity* **3**, 189 (1990). ^{139}La NQR anomalies similar to those in $\text{La}_{2-x}\text{Sr}_x\text{CuO}_4$ were also reported for $\text{La}_{2-x}\text{Ba}_x\text{CuO}_4$ and used to draw a tentative phase diagram similar to the one presented here: I. Watanabe *et al.*, *J. Phys. Soc. Jpn.* **59**, 1932 (1990), and references therein.
- [3] D. R. Harshman *et al.*, *Phys. Rev. B* **38**, 852 (1988).
- [4] B. J. Sternlieb *et al.*, *Phys. Rev. B* **41**, 8866 (1990).
- [5] M. E. Filipkowski, J. I. Budnick, and Z. Tan, *Physica (Amsterdam)* **167C**, 35 (1990).
- [6] S. M. Shapiro *et al.*, *Physica (Amsterdam)* **137B**, 96 (1986), and references therein.
- [7] A. Aharony *et al.*, *Phys. Rev. Lett.* **60**, 1330 (1988).
- [8] J. H. Cho, F. C. Chou, and D. C. Johnston, *Phys. Rev. Lett.* **70**, 222 (1993).
- [9] H. Nishihara *et al.*, *J. Phys. Soc. Jpn.* **56**, 4559 (1987).
- [10] C. Y. Chen *et al.*, *Phys. Rev. B* **43**, 392 (1991), and references therein.
- [11] C. Rettori *et al.*, *Phys. Rev. B* **47**, 8156 (1993).
- [12] Y. J. Uemura *et al.*, *Physica (Amsterdam)* **153-155C**, 769 (1988).
- [13] For a review, see D. C. Johnston, *J. Magn. Magn. Mater.* **100**, 218 (1991).
- [14] Y. Endoh *et al.*, *Phys. Rev. B* **37**, 7443 (1988); B. Keimer *et al.*, *ibid.* **45**, 7430 (1992).
- [15] M. R. McHenry, B. G. Silbernagel, and J. H. Wernick, *Phys. Rev. B* **5**, 2958 (1972).
- [16] C. P. Lindsey and G. D. Patterson, *J. Chem. Phys.* **73**, 3348 (1980). Note that an exponential \sqrt{t} behavior results quite generally from the superposition of exponentials. Therefore the observed exponential \sqrt{t} dependence of the transverse magnetization recovery is also consistent with a distribution of T_2 values.
- [17] M. C. Chen and C. P. Slichter, *Phys. Rev. B* **27**, 278 (1983).
- [18] R. J. Gooding, *Phys. Rev. Lett.* **66**, 2266 (1991); (private communication); R. J. Gooding and A. Mailhot, *Phys. Rev. B* **44**, 11 852 (1991); (to be published).
- [19] M. A. Ivanov, V. M. Loktev, and Yu. G. Pogorelov, *Zh. Eksp. Teor. Fiz.* **101**, 596 (1992) [*Sov. Phys. JETP* **74**, 317 (1992)].